Design of Field Layout for Central Receiver System to Generate 100–150 kW Solar Thermal Power

Pedamallu V.V.N.S.P. Raju and V. Narayanan

Abstract In harvesting Solar Energy via, solar thermal power, design of optical field layout is one of the important parameter for efficient land usage and also optimizing the field for energy efficiency available in a given region. Thus, in concentrated solar power (CSP) we investigate a procedure for the design and optimization of heliostat field layout for a thermal power 100–150 kW having 5–7 operational hours. First, in the design of heliostat for a given power requirement, we propose the position of the heliostat, along with curvature and dimension of the heliostat. Second, for the optimal layout, shadow lengths, altitude, and azimuthal angles were considered along with different seasons at different times with respect to Jodhpur location latitude and longitude angles. The position of the heliostat were considered, which gives minimum cosine losses. The total number of heliostat considered were ranging from 50 to 60, having varying curvature depending on its distance from the receiver, were used in the layout design. Each mirror having 6.25 m^2 area and are approximately arranged in the field of 0.57 acres area of land. The field layouts are discussed in details in terms of blocking and shadowing effects. Finally, a proposed layout is discussed for the application of CSP.

Keywords Thermal power · Field layout · Heliostat · Tower · Central receiver · Efficiency

P.V.V.N.S.P. Raju (✉)
Centre for Solar Energy Technology, IIT Jodhpur, Jodhpur, India
e-mail: rajeshpedamallu@gmail.com

V. Narayanan
Department of Physics, IIT Jodhpur, Jodhpur, India
e-mail: vnara@iitj.ac.in

L. Chandra and A. Dixit (eds.), *Concentrated Solar Thermal Energy Technologies*,
Springer Proceedings in Energy, https://doi.org/10.1007/978-981-10-4576-9_5

1 Introduction

Large-scale solar fields are used to collect the solar radiation with help of reflectors and concentrate the radiation to attain high temperatures in the receiver. A suitable mechanism is employed to convert the available high temperature at the receiver to produce electricity [1]. Among the various types of concentrating the solar radiation, the Central receivers with heliostats (mirrors) are regularly deployed [2]. In central receiver systems, high concentration of solar irradiation can be achieved thus resulting in extremely high temperature. These systems are characterized for large power levels (1–500 MW) and high temperatures (500–800 °C). Central receiver systems are based on a field layout of individual two axes Sun-tracking mirrors (heliostats). Mirrors reflect the incident solar radiation to the receiver at the top of a centrally located tower. Generally, central receiver systems are made up of heliostats, towers, receivers, heat transfer devices, thermal storage devices, and power generation parts. Further, design of solar filed depends on power requirement with available radiation in the given region. In this work, the central receiver system field layout has been designed for Jodhpur location having annual average of Direct Normal Irradiance (DNI) in Rajasthan (Jodhpur) is approximately 5.5 kWh per square meter per day [3, 4]. Accordingly, the proposed 150 kW thermal power for the Jodhpur location, we suggest the size of each heliostat having area of 6.25 m^2 with 50–60 heliostats can generate suggested power requirements with optimal land use.

2 Optical Field Efficiency

The performance of the heliostat field defines in terms of optical efficiency. It is defined as the ratio of the net power intercepted by the receiver to the power incident normally on the field [5]. Various types of losses affect the optical efficiency. The types of loss are as follows: mirror losses, atmospheric losses, spillage losses, cosine losses, shadowing, and blocking losses; which reduce the optical efficiency of the heliostat field. The optical efficiency of the field can be given by [6]:

$$\eta_{\text{field}} = \eta_{\text{mirror}} \times \eta_{\text{atm}} \times \eta_{\text{spillage}} \times \eta_{\text{cosine}} \times \eta_{\text{S\&B}} \tag{1}$$

where η_{mirror} is the efficiency of mirror reflectivity, η_{atm} is atmospheric efficiency, η_{spillage} is spillage efficiency, η_{cosine} is cosine efficiency and $\eta_{\text{S\&B}}$ is shadowing and blocking efficiency. These efficiencies are explained in the proceeding section.

2.1 *Efficiency of Mirror η_{mirror}*

Efficiency of the mirror depends upon the reflectivity of the heliostat mirrors. It completely depends on which type of material coated on backside of the mirror.

Heliostat mirror surfaces reflect most of the incident radiation but it also absorbs a portion of energy. Currently, 80–95% reflectivity mirrors are commercially available [7] and a standard value for the reflectivity 88% is considered in this field design [8].

2.2 Efficiency of Atmosphere η_{atm}

A portion of the solar radiation of the reflected rays are scattered and absorbed by the atmosphere and all the reflected solar radiation would not reach the receiver. This loss is referred as atmospheric attenuation loss. The atmospheric attenuation loss is a function of distance d_{HM} between each heliostat mirror and the receiver. The atmospheric efficiency can be expressed as [9]:

When $d_{HM} \leq 1000$ m,

$$\eta_{\text{atm}} = 0.99321 - 1.176 \times 10^{-4} d_{HM} + 1.97 \times 10^{-8} d_{HM}^2 \tag{2}$$

When $d_{HM} > 1000$ m,

$$\eta_{\text{atm}} = \text{e}^{-0.0001106 \times d_{HM}} \tag{3}$$

2.3 Spillage Efficiency $\eta_{spillage}$

All the portion of the reflected radiation cannot hit the receiver, their by causing Spillage (e.g., parameters like curvature errors, tracking errors, receiver size, etc., influence the spillage). The reflected light rays are limited due to the finite size of the receiver. The size of the aperture of the receiver is minimized to reduce the convection and radiation losses without blocking out too much of solar flux arriving at the receiver. The aperture size of the receiver is typically the same size as the Sun's reflected image from the farthest heliostat to reduce the spillage losses.

2.3.1 Curvature and Size of the Reflected Image of Concave Mirror

The radius of curvature of the mirror '*R*' is the radius of the mirror that forms a complete sphere and the focal length of the mirror '*f*' is the distance between the center of the mirror and the point at which the reflected light meets the principle axis of the mirror.

From Fig. 1, *AB* is incident light ray and *BF* is reflected light ray. *BC* represents the radius of the mirror. The line *BC* bisects the angle *ABF* and *ΔBCF* forms an isosceles triangle. Therefore, the line *BF* and *FC* are equal. We also know that *BF* and *OF* are equal for lenses that are small.

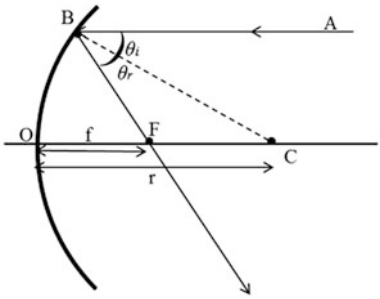

Fig. 1 Relationship between f and r for a concave mirror

$$\begin{aligned} &\therefore BF = FC = OF \;\&\\ &OC = OF + FC\\ &\Rightarrow OC = OF + OF\\ &\Rightarrow OC = 20F \Rightarrow 2F \end{aligned} \tag{4}$$

From above equations, we can say that radius of curvature of the concave mirror $OC(r)$ is equal to twice the focal length of the mirror.

$$r = 2f \tag{5}$$

Each point on a mirror will reflect a cone of rays that matches the angular distribution of the solar source (half-angle of solar rays divergence θ_s = 4.65 milli radian) [2]. The rays from the rim of the mirror will forms the widest spot on the flat target placed at the focal plane of the mirror.

From Fig. 2, the spot size 'd' can be written as

$$d = \frac{2p \sin \theta_s}{\cos \theta_R} \tag{6}$$

where 'a' is the aperture size of the mirror. When received incidence angle θ_R is small p is approximately equal to f, then image spot size being

$$d = \frac{2f \sin \theta_s}{\cos 0} = 2f \sin \theta_s \tag{7}$$

't' is the thickness or sag of the mirror. From the Sag equation we can measure the thickness 't' as

$$t = r - \sqrt{r^2 - (a/2)^2} \tag{8}$$

where 'r' is the radius of curvature of the mirror.

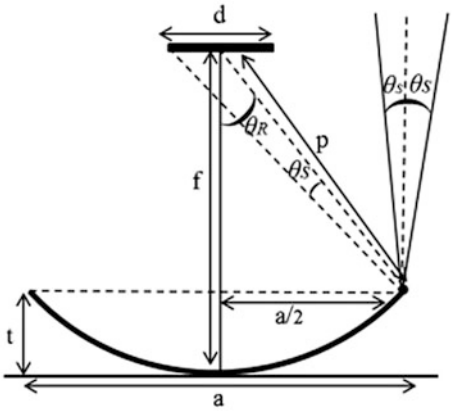

Fig. 2 Spot size of a heliostat mirror

2.4 Cosine Efficiency η_{cosine}

The cosine efficiency depends on both Sun's position and location of the individual heliostat mirrors with respect to the receiver. It is related to the cosine angle between the incident Sun ray vector and normal vector of the heliostat mirror [10]. The effective reflected area of the mirror related by cosine angle. Larger cosine angles reduce the effective reflection area.

Heliostat A has small cosine losses compared to heliostat B as shown in Fig. 3. The efficient performance of the heliostats is achieved by keeping heliostats in north side of the tower, wherein heliostats are opposite to sun. During morning hours, North West field heliostats with respect to the tower having more efficiency compared to North East field heliostats and evening time it is opposite to the field. The cosine angle between the Sun vector and the reflected vector from mirror to receiver 2θ can measure by using Sun and Earth geometry and the cosine angle 'θ' represents the cosine efficiency of the Heliostat mirror (Fig. 4).

$$\cos 2\theta = S.r \tag{9}$$

where 'S' is sun ray vector and 'r' is the reflected ray unit vector from mirror to receiver.

Sun unit vector expressed in terms of altitude and azimuth angle as [11]:

$$S = S_z i + S_e j + S_n k \tag{10}$$

where

$$\begin{aligned} S_z &= \sin\alpha \\ S_e &= \cos\alpha \sin A \\ S_n &= \cos\alpha \cos A \end{aligned} \tag{11}$$

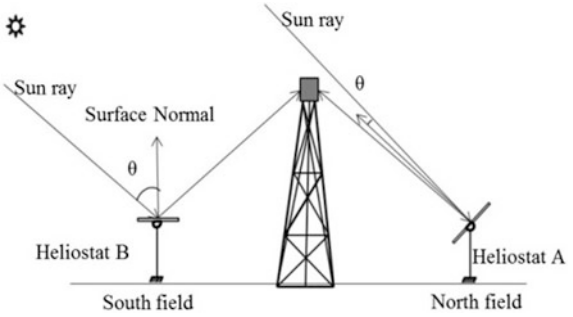

Fig. 3 The cosine effect for two heliostats in opposite directions from the tower

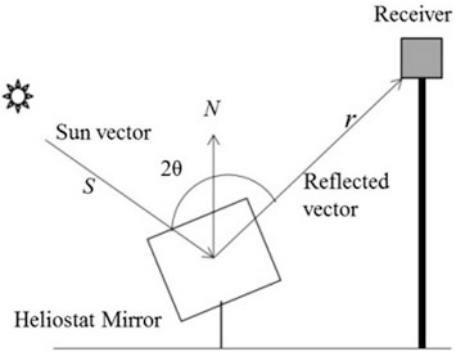

Fig. 4 The cosine angle between the heliostat to the receiver

α is altitude angle and A is the azimuth angle. Reflected ray unit vector can be written as

$$r = \frac{(x_r - x_m)i + (y_r - y_m)j + (z_r - z_m)k}{\sqrt{(x_r - x_m)^2 + (y_r - y_m)^2 + (z_r - z_m)^2}} \tag{12}$$

2.5 *Shadowing and Blocking Efficiency* $\eta_{S\&B}$

The reflected radiation from heliostat mirrors are blocked by adjacent heliostats while concentrating on to the receiver and incoming solar radiation is obstructed by the neighboring heliostats cause the shadowing effect. Shadowing and blocking effects plays a crucial role in optimized field lay out design. These effects reduce the solar radiation reaching the receiver. The amount of shadowing and blocking is a function of Sun's position angles, tower height, and heliostat mirror location in the field. When a heliostat is placed in between the two heliostats in the adjacent row, the reflected light rays can pass between the adjacent heliostats on the way to the receiver with minimal blocking effect. Shadowing and blocking efficiency can

maximize by increasing the separation between heliostats, but it consumes the more land area. We maximize the efficiency by using minimum land area in such a way that the minimum distance between two adjacent heliostats equal to the characteristic diameter (DM) of each heliostat, this is equal to the diagonal of the heliostat plus the separation distance, i.e., [5]

$$\mathrm{DM} = \mathrm{LH}\left(\sqrt{1+f^2} + ds\right) \tag{13}$$

where 'f' is the heliostat width to length ration and 'ds' is the ratio of heliostat separation distance to heliostat length (Fig. 5).

For no blocking, the minimum value of 'ds' and 'DM' as given by Collado and Turegano [12] is

$$ds_{\min} = 2f - \sqrt{1+f^2} \tag{14}$$

Therefore,

$$\mathrm{DM}_{\min} = 2\mathrm{WH} \tag{15}$$

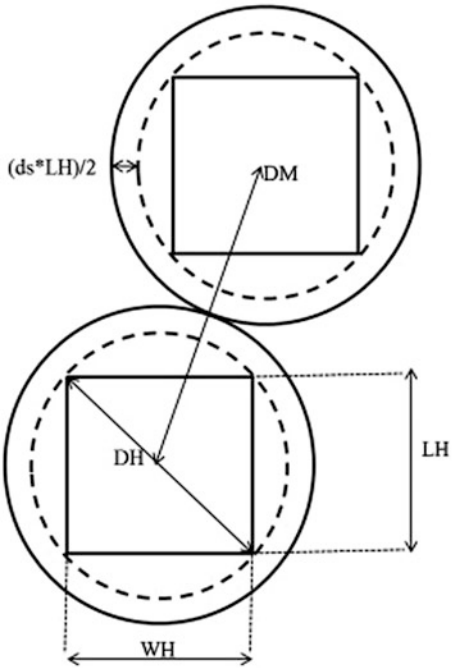

Fig. 5 Minimum distance between adjacent heliostats

Knowing of Sun's position is very important in predicting the length and direction of a shadow of the heliostat. Since Sun's light travels in straight line, the projected shadows on the ground can be measured using simple geometry.

Figure 6 shows a heliostat on a horizontal surface and 'α' is the altitude angle of the Sun's rays making with the horizontal surface. In this case, the length of the shadow can be expressed as:

$$L = h/\tan\alpha \tag{16}$$

where 'h' is the height of the mirror and Fig. 7 gives the shadow length in case of inclined plane. It can be expressed as [13]:

$$A_h = \sin\beta\cot\alpha - \cos\beta \tag{17}$$

where 'β' is the inclined plane angle and 'α' is altitude angle of Sun's rays making with horizontal surface. Altitude angle and azimuth angle gives the length and direction of the shadow.

The optical efficiency of the heliostat caused by shadowing and blocking effect are computed using ray-tracing technique. The reflective area of the test heliostat involved in the shadowing and blocking as represented in Figs. 8 and 9, respectively.

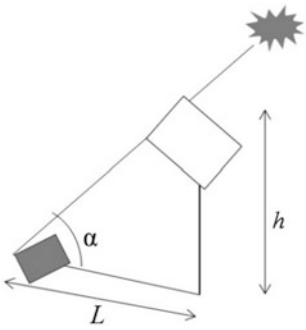

Fig. 6 Projection of vertical plane on a horizontal surface

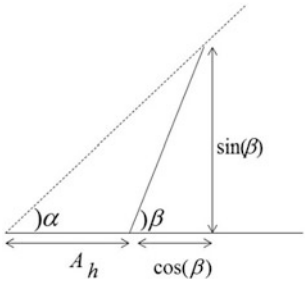

Fig. 7 Projection of inclined plane on a horizontal surface

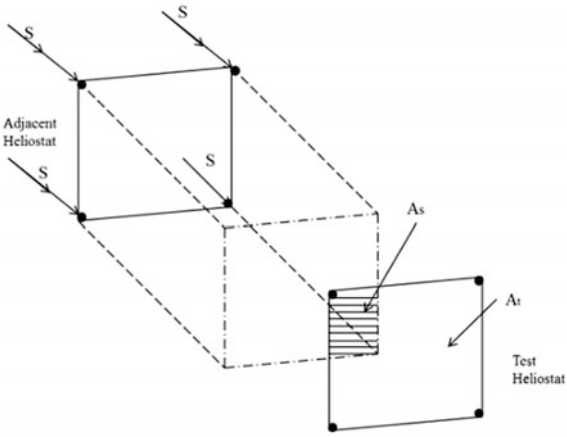

Fig. 8 Shadowing effect

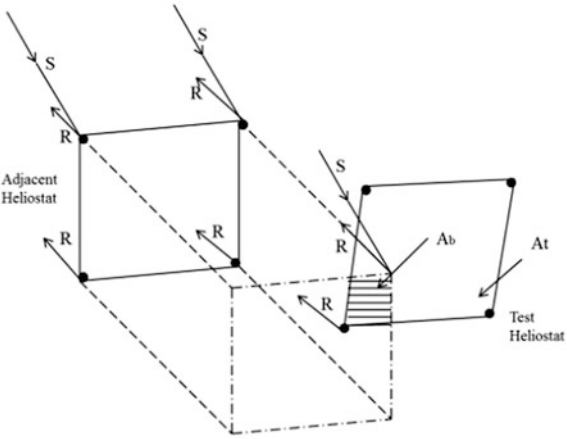

Fig. 9 Blocking effect

'A_t' is the area of the Test heliostat, 'A_s' is the shadowing area caused by the adjacent heliostat and 'A_b' is blocking area on Test heliostat due to blocking of some reflected sun rays by the adjacent heliostat. The shadowing efficiency and blocking efficiency can be calculated using below relations after finding the shadowing and blocking areas using ray-tracing techniques [14].

$$\eta_{\text{Shadow}} = \frac{(A_t - A_s)}{A_t} \tag{18}$$

$$\eta_{\text{Block}} = \frac{(A_t - A_b)}{A_t} \tag{19}$$

3 Optimized Field Layout Design

Closely packed heliostat field exhibits more shadowing and blocking losses. In general, a radial stager pattern [15] is used to minimize the land usage as well as blocking and shadowing losses. The heliostats are closely packed near the tower but those heliostats should be separated to prevent mechanical interference by the adjacent mirrors. The azimuthal spacing increases when heliostats located farther distance from the tower. Additional heliostats are added when azimuthal spacing become too large in outer rings and a new stager pattern is established.

Figure 10 shows an optimized field layout design. In this pattern, two types of rings are defined as essential rings and staggered rings. The rings which have heliostats on the north axis are called essential rings (E_1, E_2, E_3, E_4, E_5, E_6) while in staggered rings (S_1, S_2, S_3, S_4, S_5), the rings which don't have heliostats on the north axis in the field [6]. The distance between the essential or staggered rings called radial spacing 'ΔR' and the separation between heliostat in the same rings is called azimuthal spacing 'ΔA'. These two parameters defined as [15]:

$$\Delta R = HM(1.44\cot\theta_L - 1.094 + 3.068\theta_L - 1.1256\theta_L^2) \tag{20}$$

$$\Delta A = \mathrm{WM}(1.749 + 0.6396\theta_L) + \frac{0.2873}{\theta_L - 0.04902} \tag{21}$$

where HM and WM are the height and width of the heliostat, and the angle θ_L is the altitude angle to the receiver from the heliostat location and defined as [15]:

$$\theta_L = \tan^{-1}(1/R_0) \tag{22}$$

where R_0 is the radius of the first essential ring in terms of the tower height H_T.

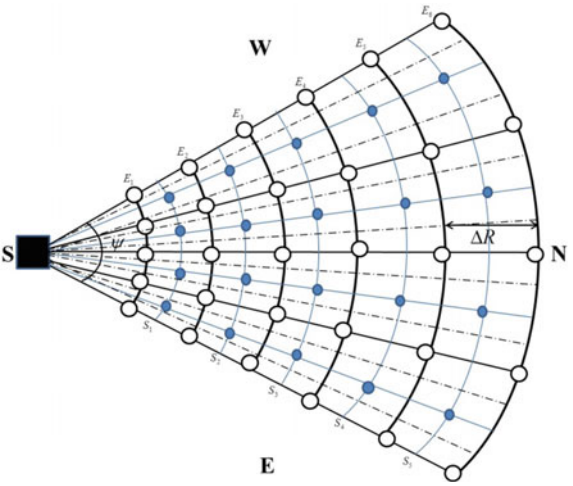

Fig. 10 The radial stagger heliostat layout pattern

According to this azimuthal distance five heliostats kept in the first ring and in the same angular direction 25 heliostats are placed in the next five essential rings (*E*). In between six essential rings, five staggered rings are there and each ring contains four heliostats in between two the adjacent essential rings. In this manner, 50 heliostats are placed in the field. Some additional heliostats can be added in between these heliostats where azimuthal spacing becoming too large in the outer rings.

4 Analysis of the Heliostat Field

The designed optimized field layout is shown in Fig. 10. The proposed height and width of the heliostat is 2.5 × 2.5 m^2 is chosen and heliostats kept at 1.5 m height from the surface of the ground (HM equal to 4 m height) minimizing the dust deposition on the mirrors. Height of the tower H_T is taken 18 m and the first essential ring radius R_0 kept as equal height of the tower. The field occupies 0.57 m^2 acres land area with the rim angle of 76.63° (field view of the receiver aperture). The required field area is calculated with different radius of essential ring R_0 and height of the tower H_0 and measured radial spacing, azimuthal spacing, rim angle of the field, and occupied field areas are mentioned in Table 1.

From the above tabular column, the increment in the rim angle ψ (field of view of the receiver aperture) and field area with decrement in the radius of the first essential ring R_0 is observed. In literature, it is reported cavity receivers or volumetric receivers are limited by an acceptance angle 60–120° [16]. Therefore, multiple cavities are placed adjacent to each other or the heliostat field is limited to the view of the cavity aperture acceptance angle [16]. When the radius of the first essential ring R_0 is 10 m, field of view (rim angle ψ) 146° exceeding the limit of acceptance angle

Table 1 The calculated field area at different radius of essential ring R_0 and different height of the tower H_0

S. No.	Height of the tower H_0 (m)	Radius of the first essential ring R_0 (m)	Radial spacing ΔR (m)	Azimuthal spacing for first ring ΔA_1 (m)	Rim angle of the field ψ (°)	Area of the field (m^2)	Field in terms of acres
1	18	10	6.78	6.36	146	2449	0.6
2	18	13.5	7.45	6.18	105	2358	0.583
3	18	15	7.72	6.12	93.56	2343.9	0.58
4	18	18	8.25	6.02	76.63	2345	0.57
5	20	18	7.93	6.07	77.37	2243.98	0.56
6	25	18	7.35	6.206	79	2068.68	0.511
7	30	18	6.94	6.31	80.37	1949.79	0.482
8	35	18	6.63	6.4	81.47	1859.34	0.4595
9	20	20	8.25	6.02	68.96	2256.07	0.56
10	30	30	8.25	6.02	45.98	2035.48	0.503

Table 2 Specifications of heliostat field and optical field efficiency

Parameters	Specifications
Total number of heliostats Height of the tower H_0	50 18
Radius of the first essential ring R_0	18 m
Total reflective area of the heliostat field	312.5 m^2
Aperture size of the receiver	0.57 m
Mirror efficiency	0.88
Atmospheric efficiency	0.9887
Spillage efficiency (in the absence of tracking and curvature errors of Heliostat mirrors)	1
Shadowing and blocking efficiency	0.92
Cosine efficiency	0.9104
Total field optical efficiency	0.7287

thus not suited for above said receiver. While minimum radius R_0, equal to height of the tower H_0 (First row) is inside the limit of acceptance angle and occupying minimal land usage. When height of the tower H_0 is increasing, this condition satisfying limit of acceptance angle and occupying minimum land area but due to the decrement in the radial spacing ΔR, shadowing and blocking effects are increasing and field having poor optical field efficiency. Further, when R_0 and H_0 are increasing in such a way that both the ratio should equal to 1, in this case field satisfying no blocking and shadowing conditions and occupying the minimum land area but due to the increment the in distance between mirrors to receiver, cosine losses and atmospheric losses are increasing slightly. The combination of tower height H_0 and first essential ring radius R_0 18 m is giving minimal land area and good optical efficiency. This field configuration satisfying the no blocking condition and having great shadowing, blocking efficiency and cosine efficiency. Shadowing and blocking efficiency is measured using ray-tracing techniques and cosine and atmospheric efficiencies are measured for each heliostat mirror using the relations (10 and 2). The total field optical efficiency (for 50 heliostat mirrors as shown in Fig. 10) is measured for Jodhpur location in India at the time of 10.30 am on 22 June. The optical field efficiency and some important parameters for the field mentioned in Table 2.

Thus, the proposed field layout with minimal area usage can operate 6–7 working hours with highly optical efficiency to generate 100–150 kW thermal power.

5 Conclusions

The optimized solar field design for heliostat and central tower has been investigated. The proposed heliostat field design provides a valuable input for estimation of energy efficiency and optimal land usage along with larger duration of operation

in a day. The design of heliostat along with curvature and dimension of the heliostat for a given optical power requirements has been investigated by considering the optimal layout, shadow lengths, altitude and azimuthal angles for given location (Jodhpur). Further, by positioning the heliostat, we find our design which gives minimum cosine losses and also, the effect with different seasons at different times for given location is investigated by location's latitude and longitude angles. A procedure for the design and optimization of heliostat field layout for a thermal power 100–150 kW having 5–7 operational hours has been reported with minimal land usage. Finally, a proposed layout is discussed for the application of CSP.

Acknowledgements The authors are thankful to MNRE and Indian Institute of Technology Jodhpur for their encouragement and financial support.

References

1. M.A. Mustafa, S. Abdelhady, A.A. Elweteedy, Analytical study of an innovated solar power tower (PS10) in Aswan (Mechanical Power Engineering Department, M.T.C., Cairo, Egypt). Int. J. Energy Eng. **2**, 273–278 (2012)
2. K. Lovegrove, W. Stein, *Concentrating Solar Power Technology, Principles, Developments and Applications* (Woodhead Publishing Series in Energy, 2012)
3. A. Kumarankandath, N. Goswami, *The State of Concentrated Solar Power in India* (Centre for Science and Environment, 2015)
4. P.R. Arora, A vital role of concentrating solar power plants of Rajasthan in future electricity demand of India (Research Scholar). Int. J. Sci. Res. Publ. **3**(6) (2013). ISSN 2250-3153
5. F.M.F. Siala, M.E. Elayeb, Mathematical formulation of a graphical method for a no-blocking heliostat field layout (Center For Solar Energy Studies, P.O. Box 12932, Tripoli, Libya). Renew. Energy **23**, 77–92 (2001)
6. Y. Zhou, Y. Zhao, in Heliostat Field Layout Design Solar Tower Plant Based on GPU. Department of Control Science and Engineering, Zhejiang University, China. *19th IFAC World Congress Cape Town, South Africa*, 24–29 Aug 2014
7. M. DiGrazia, G. Jorgensen, *Reflectech Mirror Film: Design Flexibility and Durability in Reflecting Solar Applications*. ReflecTech, Inc. Arvada, CO 80007 USA and National Renewable Energy Laboratory (2010)
8. S.A. Rafeq, Z.M. Zulfattah, A.M. Najib, M.Z.M. Rody, S. Fadhli, M.F.B. Abdollah, M.H.M. Hafidzal, Preliminary study of CST in Malaysia based on field optical efficiency (Faculty of Mechanical Engineering, Universiti Teknikal Malaysia Melaka, 76100 Durian Tunggal, Melaka, Malaysia, ScienceDirect). Procedia Eng. **68**, 238–244 (2013)
9. M. Ewert, O. Navarro Fuentes, *Modelling and Simulation of a Solar Tower Power Plant*. Master Students of Computer Science at RWTH Aachen University, Aachen, Germany (2015)
10. F. Eddhibi, M. Ben Amara, M. Balghouthi, A. Guizani, Optical study of solar tower power plant (Thermal Process Laboratory, Research and Technology center of Energy P.B $N^{0}95$ 2050, Hammam Lif-Tunisia). J. Phys. Conf. Ser. (IOP Publishing Ltd) **596**, 012018 (2015)
11. H.M. Woolf, *On the Computation of Solar Evaluation Angles and the Determination of Sunrise and Sunset Times*. National Aeronautics and Space Administration Report NASA TM-X-164, September (1968)
12. F.J. Collado, J.A. Turegano, Calculation of the annual thermal energy supplied by a defined heliostat Field. Sol. Energy **42**, 65–149 (1989)

13. D. Baldocchi, *Lecture 7, Solar Radiation, Part 3, Earth-Sun Geometry*. Department of Environmental Science, Policy and Management, University of California, Berkeley CA94720, 10 September 2012
14. K.K. Chong, M.H. Tan, Comparison study of two different sun-tracking methods in optical efficiency of heliostat field (Faculty of Engineering and Science, Universiti Tybjy Abdul Rahman, Off Jalan Genting Kelang, Setapak, 53300 Kuala Lumpur, Malaysia). Int. J. Photoenergy **2012** (2012)
15. T.A. Dellin, M.J. Fish, C.L. Yang, *A User's Manual for DELSOL2: A Computer Code for Calculating the Optical Performance and Optimal System Design for Solar Thermal Central Receiver Plants*. Sandia National Labs Report SAND81-8237, August (1981)
16. K.W. Battleson, *Solar Power Tower Design Guide: Solar Thermal Central Receiver Power Systems, A Source of Electricity and/or Process Heat*. Sandia National Labs Report SAND81-8005, April (1981)